Power System Dynamic Analysis Using Quantum Linear Differential Equation Solver Oracle

Huynh T. T. Tran*, Anh Phuong Ngo*, and Hieu T. Nguyen
Department of Electrical and Computer Engineering,
North Carolina Agricultural and Technical State University, Greensboro, NC, USA, 27411
Email: htran@aggies.ncat.edu, ango1@aggies.ncat.edu, htnguyen1@ncat.edu

2024 IEEE Power & Energy Society General Meeting (PESGM) | 979-8-3503-8183-2/24/$31.00 ©2024 IEEE | DOI: 10.1109/PESGM51994.2024.10688522

***Abstract*—This paper presents a quantum computing framework to solve a system of nonlinear ordinary differential equations (ODEs) used in the power system dynamic analysis. The framework exploits the linearization of power system dynamics' nonlinear ODEs at particular points of state variable vector to construct a system of linear ODEs (LDE) modeling the system dynamics around considered points within a small time interval. The analytical solution of this LDE system in the matrix exponential form can be simulated and transformed into quantum states using the popular design of a Variational Quantum Circuit (VQC) acting as a quantum LDE solver oracle. The oracle can be used repeatedly to construct the trajectory of the original nonlinear power system dynamics along the time evolution. Obtained numerical results using Julia-based simulatable quantum circuits demonstrate that we can tailor and leverage recent advances in quantum computing algorithms, originally designed for linear systems, to model nonlinear power system dynamics with high accuracy.**

***Keywords*—Power system dynamics, quantum linear differential equation solver, quantum computing, nonlinear ODEs.**

I. Introduction

Power system dynamic analysis is a challenging research task due to the large number of interconnected components such as generators, loads, and transmission lines along with the nonlinear nature of ordinary differential equations (ODEs) modeling system dynamics [1]. Classical computing methods, such as Euler, Runge-Kutta, and backward differentiation formula, are based on numerical discretization approaches [2] and might not scale well with the exponential increase of the system complexity induced by the growing penetration of distributed energy resources. Thus, there is an urgent need for a computationally effective approach with high solution accuracy for modern power system dynamic analysis [2].

Quantum computing as a novel computation method enables superior scaling with certain complex problems, such as linear algebra and matrix exponential calculations [3]. One application with proven quantum advances is solving linear equations. The most well-known quantum linear algebraic equation solver is the Harrow-Hassidim-Lloyd (HHL) algorithm [4]. The work [5] expanded the capability of quantum linear algebraic equation solvers, allowing them to handle high-dimensional linear systems. This is accomplished by proportionally setting the quantum states to the solution of the block-encoded N-dimensional system of linear equations, unlocking the potential for rapid characterization of solutions to high-dimensional linear systems. The work [6] presents an alternative linear equation solver using the variant of adiabatic quantum computing (AQC) for solving linear equations. By modeling a multi-step forward difference method as a system of linear equations, the work [7] showed that linear differential equations (LDEs) can be also solved effectively using the HHL circuit. The work [8] employs a quantum variational circuit (VQC) to solve the LDEs. Different from the HHL method, the VQC simulates directly the analytical solutions of LDEs, which are in matrix exponential forms and can be computed in quantum computers effectively via truncated Taylor series.

While existing quantum algorithms have succeeded in solving linear equations, both algebraic and differential forms, they cannot be applied to solve nonlinear ODEs for power system dynamics analysis. This paper presents a quantum computing approach to address the problem of solving nonlinear ODEs arising in power system dynamic analysis. We exploit the fact that the nonlinear dynamics of power systems around a particular point with a small time step of evolution can be linearly approximated and the resulting LDEs can be computed effectively using recent advances in quantum LDE solver. Among different quantum LDE solvers, such as the AQC method [6], which is costly to realize, and the HHL-based method [7], which is susceptible to noises, we choose VQC since it is resilient to quantum noise errors and has high flexibility for coherence time and gate requirements, thus more suitable for Noisy Intermediate Scale Quantum devices. Within this context, we construct the VQC in accordance to [8] as an oracle for sequentially solving LDEs to construct the trajectory of the original nonlinear power system dynamics' ODEs.

The rest of the paper is as follows. Section II reviews the mathematical model of power system dynamics. Section III presents the VQC-based LDE solver oracle to solve the nonlinear systems Case studies and numerical results are presented in Section IV, and Section V concludes the paper.

II. Mathematical model

An electric power network is an interconnection of m machines in a network of n buses with an admittance matrix $\overline{Y}_N$ [1] as shown in Figure 1 (R_{si} and X'_{di} are stator resistance and the d-axis transient reactance of the generator located in node i respectively). The load at node i can be modeled as a constant

*The first two authors contributed equally. This work is supported by the Alfred P. Sloan Foundation (#10358) and the Center for Regional and Rural Connected Communities funded by the U.S. Department of Transportation.

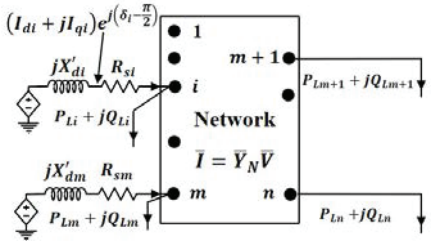

Fig. 1: Interconnection of m synchronous machine dynamic circuits and n buses with network admittance matrix $\bar{Y}_N$ [1].

impedance, particularly an admittance $\overline{y}_{Li}$, consuming power $P_{Li} + jQ_{Li}$ at a voltage magnitude V_i as follows [1]:

$$-(P_{Li} - jQ_{Li}) = \overline{y}_{Li} V_i^2 \quad \forall i = 1, \ldots, n. \tag{1}$$

Since R_{si} is generally very small and can be ignored, the network becomes an interconnection of m generation buses only as in Figure 2. This is called the internal node model with a new network equation $\overline{I}_{\text{int}} = \overline{Y}_{\text{int}} \overline{E}$. where $\overline{E}_i = E_i \angle \delta_i$ is the nodal voltage and $\overline{Y}_{\text{int}}$ is the internal node matrix constructed from network parameters such as $\overline{Y}_N$, X'_d, and $\overline{y}_L$ [1]. Then, the system dynamics (including the governor system displayed in Figure 3) can be represented as:

$$\frac{\mathrm{d}\delta_i}{\mathrm{d}t} = \omega_i - \omega_s, \tag{2a}$$

$$\frac{\mathrm{d}\omega_i}{\mathrm{d}t} = \frac{\omega_s}{2H_i}\left(T_{Mi} - P_{ei}\right), \tag{2b}$$

$$\frac{\mathrm{d}T_{Mi}}{\mathrm{d}t} = \frac{1}{T_{CHi}}\left(P_{SVi} - T_{Mi}\right), \tag{2c}$$

$$\frac{\mathrm{d}P_{SVi}}{\mathrm{d}t} = \frac{1}{T_{SVi}}(P_{Ci} - P_{SVi}) - \frac{1}{R_{Di} T_{SVi}}\left(\frac{\omega_i}{\omega_s} - 1\right), \quad \forall i = 1, \ldots, m, \tag{2d}$$

where P_{ei} is the active electrical power output of the generator:

$$P_{ei} = G_{ii} E_i^2 + \sum_{j=1, j\neq i}^{m} \Big(G_{ij} E_i E_j \cos(\delta_i - \delta_j) + B_{ij} E_i E_j \sin(\delta_i - \delta_j) \Big). \tag{3}$$

The parameters used in (2) include ω_s (the reference angular speed), H_i (the machine's initial constant), T_{CHi} (the steam chest time constant), T_{SVi} (the steam valve time constant), R_{Di} (speed regulation quantity), P_{Ci} (the power control), and $G_{ij} + jB_{ij} = \overline{Y}_{ij}$ is ij^{th} element of $\overline{Y}_{\text{int}}$. The state variables include P_{ei}, the electric power output of generator i given in (3), δ_i, the rotor angle, ω_i, the angular speed, T_{Mi}, the mechanical torque, and P_{SVi}, the steam valve position. Equations (2a) and (2b) represent the dynamic of the generators. Equations (2c) and (2d) represent the dynamic of the turbine and governor systems. Since P_{ei} is a trigonometric function of all generators' rotor angles, equation (2) indeed is a nonlinear ODE system that can be compactly rewritten as:

$$\frac{\mathrm{d}x}{\mathrm{d}t} = f(x) \tag{4}$$

where $x^\top = [x_1^\top, x_2^\top, \ldots, x_m^\top]$, $x_i^\top = [\delta_i, \omega_i, T_{Mi}, P_{SVi}]$.

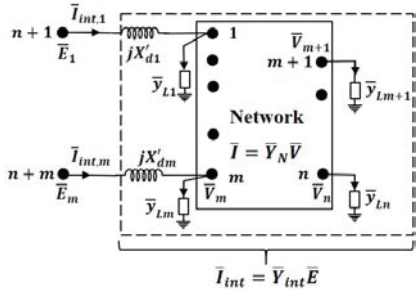

Fig. 2: Internal node model with loads as constant impedances [1].

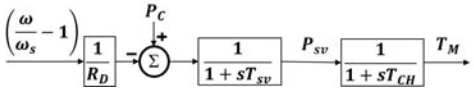

Fig. 3: Turbine and speed governor model [9].

III. Quantum Computing Approaches

A. Quantum Linear Differential Equation Solver Oracle

Consider a system of linear ordinary differential equations:

$$\frac{\mathrm{d}x}{\mathrm{d}t} = Ax(t) + b, \ t \in [0, T] \subset \mathbb{R}^+, \tag{5}$$

where $A \in \mathbb{R}^{N\times N}$ and $b \in \mathbb{R}^N$ are system matrix and vector input, and $x(t) \in \mathbb{R}^N$ is the vector of state variables, respectively. It can be solved analytically as:

$$x(t) = e^{At} x(0) + \left(e^{At} - I\right) A^{-1} b \tag{6}$$

where $x(0)$ is a vector of initial conditions. Using Taylor series, the solution $x(t)$ is approximated as:

$$x(t) \approx \sum_{m=0}^{k} \frac{(At)^m}{m!} x(0) + \sum_{n=1}^{k} \frac{A^{n-1} t^n}{n!} b, \tag{7}$$

where k denotes the Taylor polynomial's approximation order.

The equation (7) can be rewritten in terms of quantum states and operators. In particular, we can produce an operator $U = \sum_{i,j} A_{ij} |i\rangle \langle j|$ and encode $x(0)$ and b into quantum states using the probability amplitude encoding as follows [8]:

$$|x(0)\rangle = \sum_{j=0}^{N-1} \frac{x_j(0)}{\|x(0)\|} |j\rangle, \quad |b\rangle = \sum_{j=0}^{N-1} \frac{b_j}{\|b\|} |j\rangle$$

where $|j\rangle$ is the j-th computational basis vector in the Hilbert space. Using these representations, we can rewrite (7) in Dirac notations of bra and ket as follows:

$$|x(t)\rangle \approx \sum_{m=0}^{k} \underbrace{\frac{\|x(0)\|(\|(A)\|Ut)^m}{m!}}_{C_m} |x(0)\rangle + \sum_{n=1}^{k} \underbrace{\frac{\|b\|(\|(A)\|Ut)^{n-1} t^n}{n!}}_{D_n} |b\rangle \tag{8}$$

To represent the state vector $|x(t\rangle$ at time t in (8) as a quantum state, we must normalize it as follows:

$$|x(t)\rangle = \frac{1}{\mathcal{M}^2}\left(\sum_{m=0}^{k} C_m U_m |x(0)\rangle + \sum_{n=1}^{k} D_n U_{n-1} |b\rangle \right) \tag{9}$$

where $\mathcal{M}^2 = \sum C_m + \sum D_n$ is the normalization factor, and coefficients C_m and D_n are based on the initial state and the unitary operator U as given in (8).

Remark: Equation (9) represents the implementation of the analytical solution (7) in quantum computer where $x_j(t) = \mathcal{M}^2 \langle j \, | x(t) \rangle$ is the j-th element of the solution $x(t)$. In other words, since the normalized $|x(t)\rangle$ can represent a quantum state and the formulation (9) is indeed a linear expression, it can be implemented by quantum circuits, for instance, VQC.

Figure 4 represents the VQC that implements equation (9) [8]. The VQC consists of 3 layers whose resulting state vectors are denoted as $|\psi_1\rangle, |\psi_2\rangle$, and $|\psi_3\rangle$, respectively and the solution of state variable vector $x(t)$ is the output of the circuit. The operators listed in the VQC include:

$$V = \frac{1}{\mathcal{M}} \begin{bmatrix} \sqrt{\sum C_m} & \sqrt{\sum D_m} \\ \sqrt{\sum D_m} & -\sqrt{\sum C_m} \end{bmatrix} \tag{10a}$$

$$V_{S1} = \frac{1}{\sqrt{\sum C_m}} \Big[\sqrt{C_0}, \sqrt{C_1}, \ldots, \sqrt{C_k} \Big] \tag{10b}$$

$$V_{S2} = \frac{1}{\sqrt{\sum D_m}} \Big[\sqrt{D_0}, \sqrt{D_1}, \ldots, \sqrt{D_k} \Big] \tag{10c}$$

$$W_{S1} = V_{S1}^{\dagger}, \; W_{S1} = V_{S2}^{\dagger}, \; W = V^{\dagger}, \tag{10d}$$

which will be explained as follows:

The first layer employs $\log_2 N$ working qubits to encode the N-dimensional vector, 1 qubit for the first ancilla register and $log_2 k$ qubits for the second ancilla register [8]. Then, the unitary operators U_x and U_b are applied to the working qubits to create the states $|x(0)\rangle$ and $|b\rangle$ whereas V and V_{S1}/V_{S2} respectively are applied to the first and second ancilla qubits to assist the probability amplitude encoding. The resulting quantum state of the first layer is:

$$|\psi_1\rangle = \frac{1}{\mathcal{M}} \Big(|0\rangle \sum_{m=0}^{k} \sqrt{C_m} |m\rangle |x(0)\rangle + \sum_{n=1}^{k} \sqrt{D_n} |n-1\rangle |b\rangle \Big). \tag{11a}$$

In the second layer, the working qubits and the second ancilla qubit are entangled whereas a sequence of operators $U_0, U_1, \ldots, U_k$ is applied on the working qubits, consequently producing the following quantum state:

$$|\psi_2\rangle = \frac{1}{\mathcal{M}} \Big(|0\rangle \sum_{m=0}^{k} \sqrt{C_m} \, |m\rangle \, U_m \, |x(0)\rangle + |1\rangle \sum_{n=1}^{k} \sqrt{D_n} \, |n-1\rangle \, U_{n-1} \, |b\rangle \Big). \tag{11b}$$

In the third layer, operation $|0\rangle\langle 0| \otimes W_{S1} + |1\rangle\langle 1| \otimes W_{S2}$ is applied on ancilla qubits, which decodes the quantum state $|\psi_2\rangle$ to produce:

$$|\psi_3\rangle = \frac{1}{\mathcal{M}^2} |0\rangle |0\rangle^{\otimes T} \Big(\sum_{m=0}^{k} C_m U_m |x(0)\rangle + \sum_{n=1}^{k} D_n U_{n-1} \, |b\rangle \Big). \tag{11c}$$

Finally, we measure the working qubits with ancilla qubits set to $|0\rangle$, to extract the solution $|x(t)\rangle$ of the linear ODE (5).

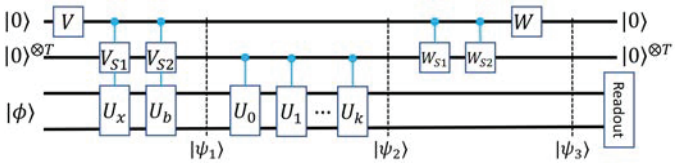

Fig. 4: VQC for quantum LDE oracle: $|0\rangle$ and $|0\rangle^{\otimes T}$ are respectively the first and second ancilla qubits, $|\phi\rangle$ are working qubits, where the initial quantum states are fed into the system (specifically, $|x(0)\rangle$ and $|b\rangle$ are generated by operators U_x and U_b) [8].

B. Solving nonlinear power system dynamics

The VQC circuit presented above can act as a quantum LDE oracle. The power system dynamics in the compact form (4), however, is nonlinear ODEs. Its linearization at a particular starting point x^* can be represented as follows:

$$\frac{\mathrm{d}\Delta(x)}{\mathrm{d}t} = J\Delta(x) + b \text{ with } \begin{cases} \Delta(x) = x(t) - x^* \\ J = \nabla_f^{\top}(x^*) \\ b = f(x^*) \end{cases} \tag{12}$$

Because we approximate the state evolution around the starting point x^*, i.e., $x(0) = x^*$, we have $\Delta x(0) = 0$ and the change of state variable x from x^* after a small time t is:

$$\Delta x(t) = \big(e^{Jt} - I\big) J^{-1} b, \tag{13}$$

The equation (13) is a special case of (6). Thus it can be solved by the VQC presented above for $\Delta x(t)$ and the new state variable at time t will be $x(t) = x^* + \Delta x(t)$. Thus, we can approximate the trajectory of $x(t)$ with the time step-size τ by sequentially performing computing $x(t_r)$ at individual time points: $t_r \in \{0, \tau, 2\tau, 3\tau \ldots\}$ using the VQC based quantum LDE oracle with $x^* = x(t_{r-1})$ and $t = \tau$.

IV. Case Studies and Numerical Results

We consider two test cases: (i) a single-machine infinite bus (SMIB) system, and (ii) the Western System Coordinating Council three-machine nine-bus (WSCC 3M9B) system, whose parameters are referred from [1] (Chapter 5 and Chapter 7, respectively). The ODEs modeling power system dynamics are implemented in Julia using the ModelingToolkit (MTK) package [10] whereas the Yao package is used as the quantum simulator [11]. We leverage the QuDiffEq package for implementing the quantum LDE oracle. We use root mean square error (RMSE) and maximum absolute error (MAE) to compare the difference between the results of classical and quantum computing-based approaches. Dashed lines represent the results of the Runge-Kutta method [12] while solid lines represent the results obtained by the Quantum LDE oracle. The complete implementation details and source code of this study are available on the GitHub repository [13].

A. Single machine infinite bus system

The SMIB system depicted in Figure 5 consists of a single generator and an extremely robust grid (infinite bus) connected by a lossless transmission line [14]. Let E_c, V denote the magnitudes of the machine's internal and the infinite bus voltages, and X_d, X_ℓ are the machine's internal and transmission line reactances. Also, T_M^0, H, D are the constant

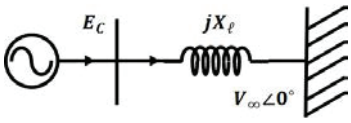

Fig. 5: Single machine infinite bus system [1].

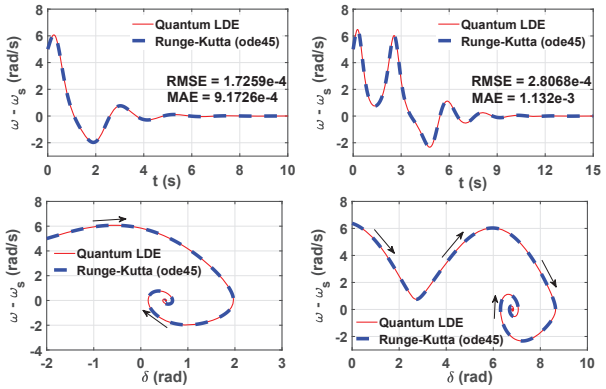

(a) Normal operation (b) Pole slipping

Fig. 6: SMIB system's results.

mechanical torque, the machine's inertial constant, and the damping constant, respectively. Thus, equation (2) becomes:

$$\frac{d\delta}{dt} = \omega - \omega_s \tag{14a}$$

$$\frac{d(\omega - \omega_s)}{dt} = K_1 - K_2 \sin(\delta) - K_3(\omega - \omega_s), \tag{14b}$$

where $K_1 = \frac{\omega_s}{2H} T_M^0$, $K_2 = \frac{\omega_s}{2H} \frac{E_c V}{X_d + X_\ell}$, $K_3 = \frac{\omega_s}{2H} D$.

We simulate the SMIB dynamics (14) with an initial transient speed of $\omega(0) - \omega_s = 5$rad/s and rotor angle of $\delta(0) = -2$rad in two scenarios: (i) normal condition with $K_1 = 5$, $K_2 = 10$, and $K_3 = 1.7$, and (ii) pole slipping conditioning (by altering K_3 to 1.5). Figure 6 shows that the system converges to the equilibrium in both scenarios where the pole slipping case has a longer transient time with a new equilibrium point (6.81rad from 0.52rad) as shown in the phase portraits. Both quantum computing and classical methods have almost identical simulation results with small errors, i.e., RMSEs of angular velocities are $1.7259 \cdot 10^{-4}$ for the normal condition and $2.8068 \cdot 10^{-4}$ for the pole slipping case. The MAEs of angular velocities are higher, as they represent the maximum error between the quantum LDE and Runge-Kutta methods, which are $9.1726 \cdot 10^{-4}$ and $1.132 \cdot 10^{-3}$, respectively.

B. WSCC three-machine nine-bus system

The WSCC three-machine nine-bus system, depicted in Figure 7, is assumed to operate normally until the demand changes at $t = 5$s. Its original equilibrium can be found in [1]. We evaluate the dynamics of the system in two scenarios:

- **Increasing demand:** demand at Bus 5 and Bus 8 increase by $0.4 + j0.2$pu, and $0.3 + 0.15$pu, respectively.
- **Decreasing demand:** demand at Bus 5, Bus 6, and Bus 8 decrease by $0.2 + j0.1$pu, $0.2 + j0.05$pu, and $0.1 + j0.1$pu.

Figure 8 illustrates the changes in the variables of three generators, i.e., transient speed $\omega_i - \omega_s$ (left column) and the phase portrait (right column) ($i = 1, 2, 3$) for generators G1, G2, G3, respectively, with Taylor polynomial approximation order is 5 and time steps is 0.01. At $t = 5$s, there is a short rise in the demand, leading to a power shortage in the system. Consequently, the angular speed of the synchronous machines decreases before becoming stable thanks to the governors' response which increases the power generation of the machine. As shown in the phase portrait, the system attains a new equilibrium point at a rotor angle lower than the initial point.

Figure 9 reveals an inverse observation when the demand drops abruptly at $t = 5$s. Since the power generated by the generators exceeds the load, its angular speed increases. The system exhibits oscillation before settling down to a new state when the transient speeds of all generators converge to zero due to the governor system's operation. In both Figures 8-9, all generators revert to the equilibrium state. It also highlights that regardless of whether the demand increased or decreased, the RMSEs and MAEs of three generators increased from generator 1 to generator 3, but remain insignificant. This demonstrates the efficiency and accuracy of the quantum LDE oracle in simulating power system dynamics.

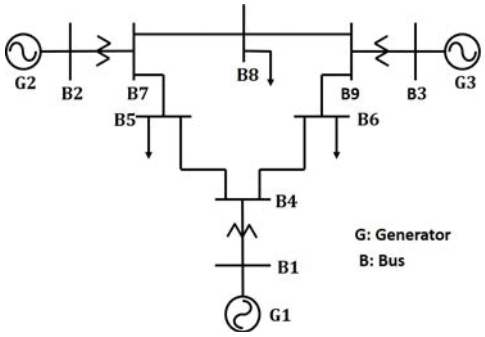

Fig. 7: WSCC three-machine nine-bus system [1].

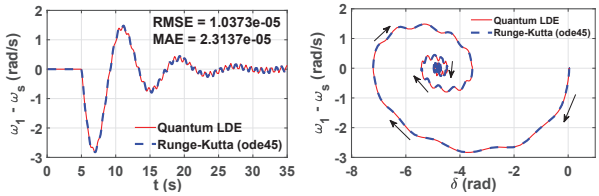

(a) Generator 1

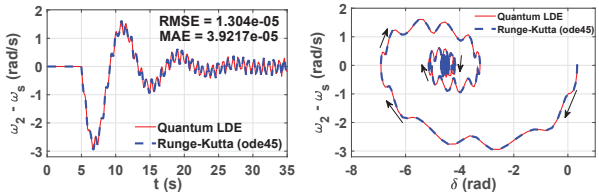

(b) Generator 2

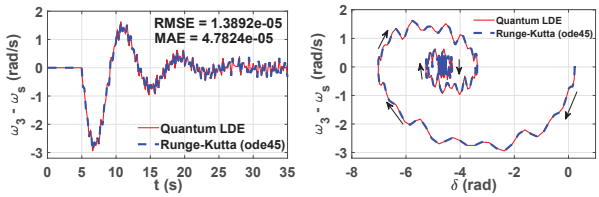

(c) Generator 3

Fig. 8: The WSCC 3M9B system with increased demand.

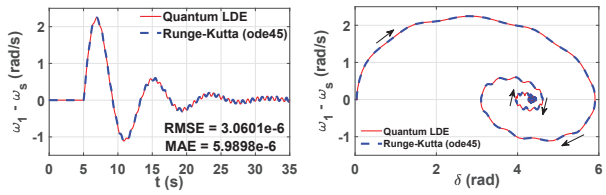

(a) Generator 1

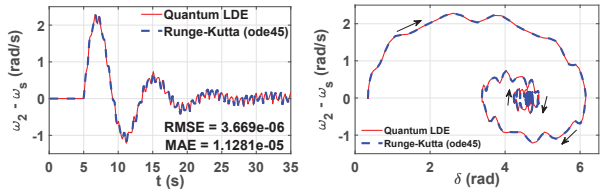

(b) Generator 2

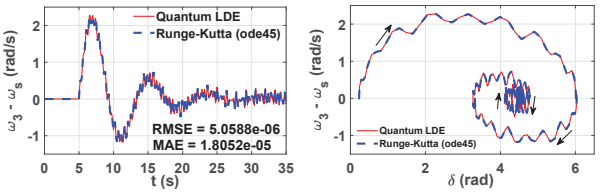

(c) Generator 3

Fig. 9: The WSCC 3M9B system with decreased demand.

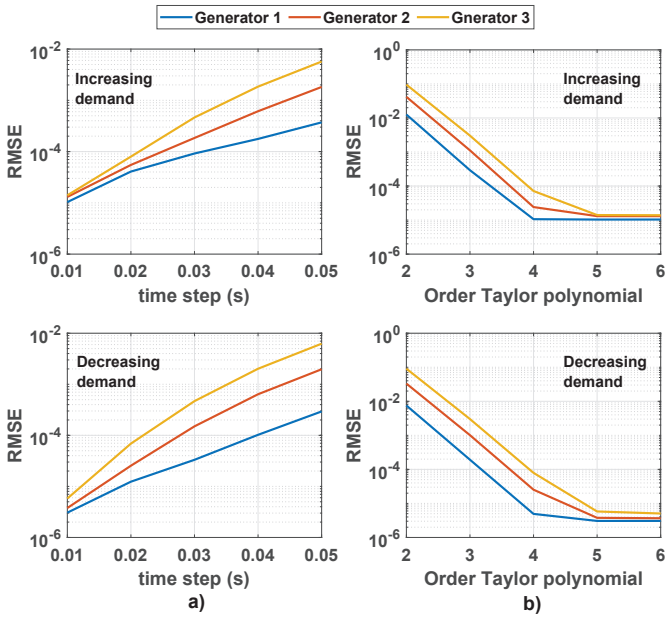

Fig. 10: Root mean square error: a) with different time steps, b) with different Taylor polynomial approximation order.

Figure 10 shows the RMSEs of two scenarios with different time steps when the order of Taylor polynomial approximation is 5 (Figure 10a) and different Taylor polynomial approximation order with 0.01-time step (Figure 10b) for all generators. It is observed that the RMSEs of all generators decrease as we reduce the time step τ or increase the order of the truncated Taylor expansion. Note that the number of qubits for the second ancilla register is equal to the logarithmic of the order of truncated Taylor polynomial [8]. It does not affect the number of qubits used to encode the N-dimensional state vector of the system dynamics, which equals $\log_2 N$. Since the number of state variables in the internal node model with m machines in equation (2) is $N = 4\times m$, we need $2+\log_2 m$ qubits for the probability amplitude encoding task.

V. Conclusion

This paper introduces a quantum computing framework for solving nonlinear ODEs in power system dynamic analysis. For small time steps, the nonlinear ODEs can be linearized as LDEs to be solved by VQC, a matured algorithm suitable for Noisy Intermediate-Scale Quantum devices. Specifically, the analytical solutions of LDEs in the matrix exponential form are computed by VQC using truncated Taylor expansion through a set of quantum operators and measurements. The VQC is sequentially employed to construct the full trajectory of the originally nonlinear ODEs modeling the power system dynamics. Our numerical results conducted on the SMIB and the WSCC three-machine nine-bus systems using Julia-based simulatable quantum circuits demonstrate the potential of modeling nonlinear power system dynamics with recent advances in quantum computing algorithms, which were originally designed for solving linear systems.

References

[1] P. W. Sauer, M. A. Pai, and J. H. Chow, *Power system dynamics and stability: with synchrophasor measurement and power system toolbox*. John Wiley & Sons, 2017.

[2] J. Stiasny, S. Chatzivasileiadis, and B. Zhang, "Solving differential-algebraic equations in power systems dynamics with neural networks and spatial decomposition," *arXiv preprint arXiv:2303.10256*, 2023.

[3] R. LaPierre, *Introduction to quantum computing*. Springer Nature, 2021.

[4] A. W. Harrow, A. Hassidim, and S. Lloyd, "Quantum algorithm for linear systems of equations," *Physical review letters*, vol. 103, no. 15, p. 150502, 2009.

[5] A. M. Childs, R. Kothari, and R. D. Somma, "Quantum algorithm for systems of linear equations with exponentially improved dependence on precision," *SIAM Journal on Computing*, vol. 46, no. 6, pp. 1920–1950, 2017.

[6] Y. Subaşı, R. D. Somma, and D. Orsucci, "Quantum algorithms for systems of linear equations inspired by adiabatic quantum computing," *Physical review letters*, vol. 122, no. 6, p. 060504, 2019.

[7] D. W. Berry, "High-order quantum algorithm for solving linear differential equations," *Journal of Physics A: Mathematical and Theoretical*, vol. 47, no. 10, p. 105301, 2014.

[8] T. Xin, S. Wei, J. Cui, J. Xiao, I. Arrazola, L. Lamata, X. Kong, D. Lu, E. Solano, and G. Long, "Quantum algorithm for solving linear differential equations: Theory and experiment," *Physical Review A*, vol. 101, no. 3, p. 032307, 2020.

[9] F. L. Alvarado, J. Meng, C. L. DeMarco, and W. S. Mota, "Stability analysis of interconnected power systems coupled with market dynamics," *IEEE Transactions on power systems*, vol. 16, no. 4, pp. 695–701, 2001.

[10] Y. Ma, S. Gowda, R. Anantharaman, C. Laughman, V. Shah, and C. Rackauckas, "Modelingtoolkit: A composable graph transformation system for equation-based modeling," 2021.

[11] X.-Z. Luo, J.-G. Liu, P. Zhang, and L. Wang, "Yao. jl: Extensible, efficient framework for quantum algorithm design," *Quantum*, vol. 4, p. 341, 2020.

[12] C. Rackauckas and Q. Nie, "Differentialequations.jl–a performant and feature-rich ecosystem for solving differential equations in julia," *Journal of Open Research Software*, vol. 5, no. 1, p. 15, 2017.

[13] H. T. Tran, P. Ngo, and H. T. Nguyen, "Code repository for this paper," 2024. [Online]. Available: https://github.com/ThanhEthan/PowerSystemDynamics_Quantum

[14] S. Wang, W. Gao, and A. S. Meliopoulos, "An alternative method for power system dynamic state estimation based on unscented transform," *IEEE transactions on power systems*, vol. 27, no. 2, pp. 942–950, 2011.